Chapter 3

Tunable Guided Wave Components using POLICRYPS Holographic Gratings

Introduction

Optical tuneable filters are essential components in the next generation Fiber-To-The-Home wavelength division multiplexing optical communication systems and in optical sensor systems. Such devices continue to stimulate an extensive research activity. The main goal of this is the realization of novel structures, characterized by compactness, low cost, high performance and low power consumption. Currently also the mature waveguide technology based on $LiNbO_3$, characterized by highly efficient electro-optic effect[24] and acousto-optic effect[25], do not allow to overcome problems of too high insertion losses, high fabrication costs, and crosstalk. The ideal material able to include efficient externally controlled light effects to perform optical modulation, optical switching and other processing functions especially in low loss channel waveguides has not realized yet. Silica on silicon is an excellent material for passive low loss integrated optic devices, whose fabrication is complex and quite expensive. Much attention has been devoted to liquid crystals (LC) and composite materials made of liquid crystal and polymers as efficient materials for photonic devices.

In general LC and composites can be considered as active materials to be combined with low loss and reliable passive waveguide technology. Main advantages in using LC are their transparency in the near infrared spectrum for any data formats, their high birefringence, with refractive index ranging between 1.4 and 1.6 as silica optical fibers and low loss optical waveguides. Furthermore mechanical integrity is relatively easy to reach because LC do not have moving parts.

3.1 Tuneable Optical Filters

Tunable optical filters (TOF) are now key components for wavelength or channel selection not only in optical communication systems using wavelength division multiplexing (WDM) techniques, but also in fiber optic video broadcast and select networks, fiber optic sensing systems, as well as optical spectrometers. However, different applications usually require different TOF characteristics, including bandwidth, tuning range, tuning speed, insertion loss, polarization dependence, stop band rejection ratio, scalability, cost, repeatability and stability.

In the past decades, a great number of different tunable filter techniques have been proposed and developed. Some of them have been extensively studied and have achieved great success, at least in WDM telecommunication networks. These tunable techniques can be categorized according to the core device being used, into Fabry-Perot TOF, mode coupling TOF, diffraction grating TOF, and other tunable filters including Mach-Zehnder interferometers, ring or disl resonators, waveguide arrays, and photonic bandgap (PBG) filters. One of the most important system is the tunable filter based on mode coupling. Coupled mode theory is a method that can be used to describe the wave behaviour in a perturbed waveguide system by means of the know normal modes of the unperturbed system.

Based on the mode coupling theory, tunable filters can be constructed using acousto-optic, electro-optic or magneto-optic effects. The principle diagram of a typical structure of a mode coupling tunable filter is shown in fig. 3.1

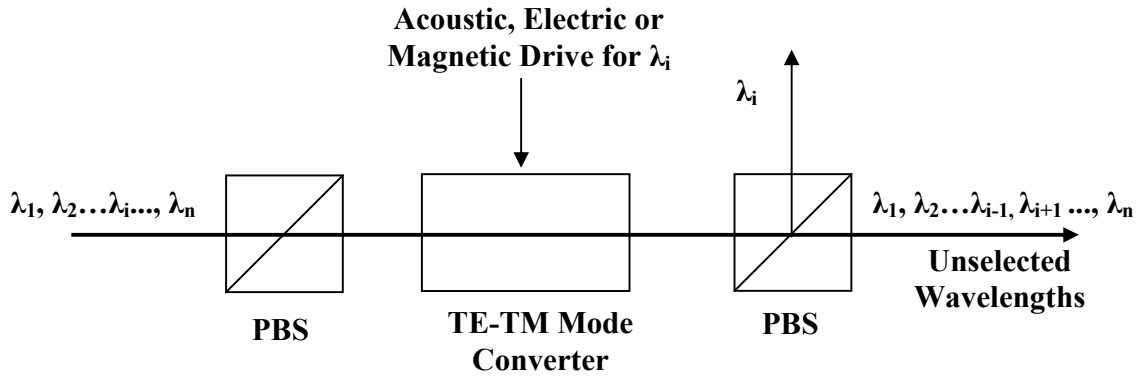

Figure 3.1: Tunable filter based on mode coupling

Acousto-optic tunable filters (AOTFs)[26,27] are the most important mode coupling tunable filters. An AOTF consists of an imput polarizer an appropriate acoustic transducer, such an x-cut LiNbO3 substrate, and an output polarizer. By changing the frequency of the acoustic waves, a corresponding optical wavelength can be selected. A typical AOTF has a bandwidth less than 1 nm, a tuning range over 100nm, and a tuning speed on the order of microseconds. The distinguished characteristics of AOFT are capability of selecting multiple arbitrary wavelength simultaneously if multiple frequency acoustic waves are applied, low operation voltage and compatibility with integrated optics. The multiple wavelength selection capability is very useful in an optical add/drop (OAD) device of WDM networks. Major disadvantages in AOTF are: expensive technology, low reliability for large area fabrication, high polarization dependence, sensitivity to temperature change and high power consumption.

3.2 Bragg Grating Filter

A Bragg grating can be loosely defined as a periodic structure that scatters radiation in a way that generates constructive interference. The concept of constructive interference and wave propagation in periodic structures arises in a variety of physical situations including periodic antenna arrays, crystal diffraction, and even the quantum mechanical interaction of electrons with semiconductor crystal. In this work we consider a very simple Bragg grating structures in which light is confined to propagate in only one dimension. The one dimensional Bragg grating is a periodic structure which coherently reflects light travelling in one direction into the opposite direction. The principle of Bragg reflection can also apply to guided wave devices. If a periodic perturbation is introduced in the dielectric medium, a portion of the incident light can be reflected into the opposite propagation direction. As with other forms of Bragg reflection the path difference between reflected light from subsequent grating periods must be an integral number of wavelengths. Strongest reflection occurs when the path difference is precisely one wavelength, meaning the grating period must be one half of the wavelength

$$\Lambda = \frac{\lambda_0}{2n_{eff}} \tag{1}$$

Here Λ is the grating period, λ_0 is the free space wavelength, and λ_0/n_{eff} is the wavelength of light inside of the dielectric material (n_{eff} is the effective index of refraction of the guiding dielectric structure).

The principle of reflection from a Bragg grating in a waveguide structure is illustrated in Fig. 3.2.

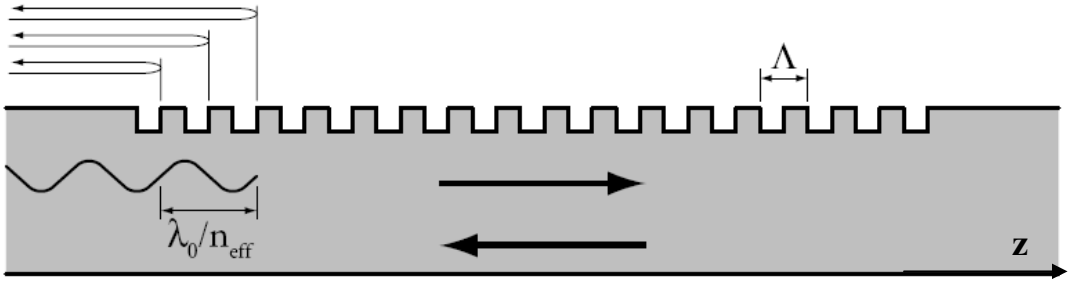

Figure 3.2: A Bragg grating constructed on the surface of an optical waveguide.

3.2.1 Coupled Mode Equations

The response of a grating can be calculated by treating the grating as a small perturbation of a otherwise normal waveguide. Rather than analyzing the reflection from each tooth of the grating separately, we instead treat the grating as a distributed reflector, parameterized by a grating strength, κ, which describes the rate at which energy is transferred between the otherwise decoupled forward and backward modes. In the absence of a grating, the propagation of light in a waveguide can be described in terms of the following equations:

$$\begin{aligned} \frac{d}{dz} a_{+}(z) &= +i\beta a_{+}(z) \\ \frac{d}{dz} a_{-}(z) &= -i\beta a_{-}(z) \end{aligned} \qquad (2)$$

where $a_{+}(z)$ and $a_{-}(z)$ represent the mode amplitudes of the forward and backward travelling waves respectively, and β is the propagation constant of the waveguide at a certain wavelength.

The Cartesian coordinate axes have been oriented such that the waveguide points in the z direction, and an implicit time dependence of $e^{-i\omega t}$ has been factored out of all quantities. Notice that in the absence of a grating structure, the equations of motion for forward and backward travelling waves are completely decoupled. The solution to equations 2 is a pair of independent travelling waves in the +z and –z directions. When a grating is added to the guiding structure the equations of motion for $a_+(z)$ and $a_-(z)$ are no longer decoupled. The modified coupled mode equations are:

$$\begin{aligned}\frac{d}{dz}a_+(z) &= +i\beta a_+(z) + \kappa e^{+iqz}a_-(z)\\ \frac{d}{dz}a_-(z) &= -i\beta a_-(z) + \kappa^* e^{-iqz}a_+(z)\end{aligned} \tag{3}$$

The first terms in these equations are identical to those of equations 2, but the second term represent the effect of the grating. In the equation 3, κ is a quantity known as the grating strength, which is a measure of how much reflection is generated per unit length along the grating and q is wave vector of the grating.

3.2.2 Solution of Coupled Mode Equations

In solving the coupled mode equations, it is useful to factor out the rapidly oscillating components from the mode amplitudes $a_+(z)$ and $a_-(z)$. The rapid oscillations are removed by making the following change of variables:

$$\begin{aligned}A_+(z) &= a_+(z)e^{-\frac{i}{2}qz}\\ A_-(z) &= a_-(z)e^{+\frac{i}{2}qz}\end{aligned} \tag{4}$$

$A_+(z)$ and $A_-(z)$ represent slowly varyng mode envelope functions, after the rapid optical oscillations have been factored out.

After making this substitution, the coupled mode equations 3 simplify to:

$$\frac{d}{dz}A_{+}(z)=+i\delta A_{+}(z)+\kappa A_{-}(z)$$
$$\frac{d}{dz}A_{-}(z)=-i\delta A_{-}(z)+\kappa^{*}A_{+}(z) \quad (5)$$

where δ is a measure of the deviation from the Bragg condition, given by

$$\delta = \beta - \frac{1}{2}q = \beta - \frac{\pi}{\Lambda} \quad (6)$$

The coupled mode equations for $A_{+}(z)$ and $A_{-}(z)$ can be written in the convenient matrix form:

$$\frac{d}{dz}\begin{bmatrix} A_{+}(z) \\ A_{-}(z) \end{bmatrix} = \begin{bmatrix} +i\delta & \kappa \\ \kappa^{*} & -i\delta \end{bmatrix}\begin{bmatrix} A_{+}(z) \\ A_{-}(z) \end{bmatrix} \quad (7)$$

Notice that after changing variables to $A_{+}(z)$ and $A_{-}(z)$, the resulting equations of motion comprise a system of coupled linear differential equations. Equation 7 is a linear vector differential equation which can be solved in the conventional way by computing the eigenvectors and eigenvalues of the system of equations. Using this method of eigenvector decomposition, the solution is:

$$\begin{bmatrix} A_{+}(z) \\ A_{-}(z) \end{bmatrix} = \begin{bmatrix} \mathbf{v_1} & \mathbf{v_2} \end{bmatrix}\begin{bmatrix} e^{\lambda_1 z} & 0 \\ 0 & e^{\lambda_2 z} \end{bmatrix}\begin{bmatrix} \mathbf{v_1} & \mathbf{v_2} \end{bmatrix}^{-1}\begin{bmatrix} A_{+}(z) \\ A_{-}(z) \end{bmatrix} \quad (8)$$

where $\mathbf{v_1}$ and $\mathbf{v_2}$ are the eigenvectors of the system and λ_1 and λ_2 are the corresponding eigenvalues.

The eigenvalues and associated eigenvectors are given by:

$$\begin{aligned} \lambda_1 &= +\gamma \\ \lambda_2 &= -\gamma \end{aligned} \tag{9}$$

$$\begin{aligned} \mathbf{v_1} &= \begin{bmatrix} i\delta + \gamma \\ \kappa^* \end{bmatrix} \\ \mathbf{v_2} &= \begin{bmatrix} -\kappa \\ i\delta + \gamma \end{bmatrix} \end{aligned} \tag{10}$$

where we have defined the quantity γ as:

$$\gamma = \sqrt{|\kappa|^2 - \delta^2} \tag{11}$$

Substituting the eigenvalues and eigenvectors from 9 and 10 into the vector solution in equation 3.8, the following simplified solution for the mode amplitudes is obtained:

$$\begin{bmatrix} A_+(z) \\ A_-(z) \end{bmatrix} = \begin{bmatrix} \cosh(\gamma z) + i\frac{\delta}{\gamma}\sinh(\gamma z) & \frac{\kappa}{\gamma}\sinh(\gamma z) \\ \frac{\kappa^*}{\gamma}\sinh(\gamma z) & \cosh(\lambda z) - i\frac{\delta}{\gamma}\sinh(\gamma z) \end{bmatrix} \begin{bmatrix} A_+(0) \\ A_-(0) \end{bmatrix} \tag{12}$$

This solution can then written in terms of the original mode amplitude quantities, $a_+(z)$ and $a_-(z)$ by using the relationships given in equations 4

$$\begin{bmatrix} a_+(z) \\ a_-(z) \end{bmatrix} = \begin{bmatrix} e^{-\frac{i}{2}k_g z} & 0 \\ 0 & e^{-\frac{i}{2}k_g z} \end{bmatrix} \begin{bmatrix} \cosh(\gamma z) + i\frac{\delta}{\gamma}\sinh(\gamma z) & \frac{\kappa}{\gamma}\sinh(\gamma z) \\ \frac{\kappa^*}{\gamma}\sinh(\gamma z) & \cosh(\lambda z) - i\frac{\delta}{\gamma}\sinh(\gamma z) \end{bmatrix} \begin{bmatrix} a_+(0) \\ a_-(0) \end{bmatrix} \tag{13}$$

3.2.3 Reflection Spectral Response of Bragg Grating

Equation 12 is a closed form solution to the coupled mode equations, which gives the mode amplitudes at any point z, given the initial forward and backward mode amplitudes at z=0. Often, the boundary conditions on $a_+(z)$ and $a_-(z)$. at z=0 are not simultaneously known. Consider a grating extending from z=0 to L, with some signal incident from the left. The two boundary conditions for this problem are that no signal is incident from the right hand side of the grating (a–(L) = 0), and that some known signal is incident from the left (a+(0) = 1.) From these two boundary conditions we wish to derive the transmission and reflection coefficients for the grating segment. Substituting these boundary conditions into the matrix equation 13 gives:

$$\begin{bmatrix} t \\ 0 \end{bmatrix} = \begin{bmatrix} e^{+\frac{i}{2}qz} & 0 \\ 0 & e^{-\frac{i}{2}qz} \end{bmatrix} \begin{bmatrix} \cosh(\gamma z) + i\frac{\delta}{\gamma}\sinh(\gamma z) & \frac{\kappa}{\gamma}\sinh(\gamma z) \\ \frac{\kappa^*}{\gamma}\sinh(\gamma z) & \cosh(\lambda z) - i\frac{\delta}{\gamma}\sinh(\gamma z) \end{bmatrix} \begin{bmatrix} 1 \\ r \end{bmatrix} \tag{14}$$

where r and t represent the amplitude reflection and transmission coefficients of the grating, respectively. Equation 14 represents two linear equations with two unknown quantities, r an t. It is straightforward to solve for r(δ) from second equation.

$$r(\delta) = \frac{\frac{\kappa^*}{\gamma}\tanh(\gamma L)}{1 - i\frac{\delta}{\gamma}\tanh(\gamma L)} \tag{15}$$

The quantities γ and δ are defined in equations 6 and 11. The case δ=0 corresponds to an incident signal whose wavelength meets the Bragg condition. When δ=0, the magnitude of the reflection coefficient simplifies to:

$$|r(\delta=0|^2 = \tanh^2(|\kappa|L) \tag{16}$$

Figure 3.3 plots the reflection spectrum $|r(\delta=0)|^2$ of a Bragg grating for several κL values.

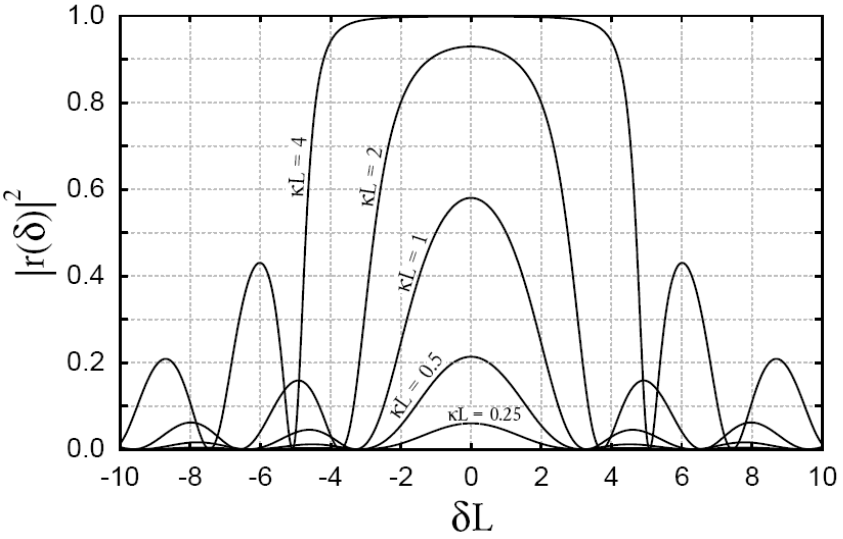

Figure 3.3: Reflection spectra from Bragg gratings with different κL values.

As we can see, for small κL values, where κL represented the deviation from the Bragg condition, the spectral response has a sinc-shaped response while for large κL the response has a plateau shape.

3.2.4 General Properties of Waveguides

The propagation of light in a waveguide is described by Maxwell's equations, which govern all electromagnetic phenomena. When describing electromagnetic propagation in lossless dielectric media, it is convenient to express Maxwell's equations in the following form:

$$\begin{aligned} \nabla \times \mathbf{E} &= ik\sqrt{\frac{\mu_0}{\varepsilon_0}}\mathbf{H} \\ \nabla \cdot \left(n^2 \mathbf{E}\right) &= 0 \\ \nabla \times \mathbf{H} &= -ikn^2\sqrt{\frac{\varepsilon_0}{\mu_0}}\mathbf{E} \\ \nabla \cdot \mathbf{H} &= 0 \end{aligned} \tag{17}$$

where **E** and **H** are the electric and magnetic fields respectively, and n(**r**) is the dimensionless index of refraction which for a waveguide is a function of position. In lossless materials n(**r**) is a positive real quantity, ε_0 and μ_0 are the permittivity and permeability of free space. We will consider only non-magnetic materials, for which $\mu=\mu_0$. The form of Maxwell's equations given in equation 4.1 applies only in source free regions of space, where there is no free current or charge (J=0 and σ=0).

A dielectric waveguide structure is completely specified by the refractive index profile n(**r**). Typically, the Cartesian axes are chosen such that the waveguide points along the z direction, meaning that n(**r**) depends only on the Cartesian coordinates x and y, but not on z

$$n(\mathbf{r}) = n(x,y) \tag{18}$$

The geometry of a uniform waveguide is described completely by the two dimensional index profile n(x,y).

Figure 3.4 illustrates one example of an optical waveguide structure:

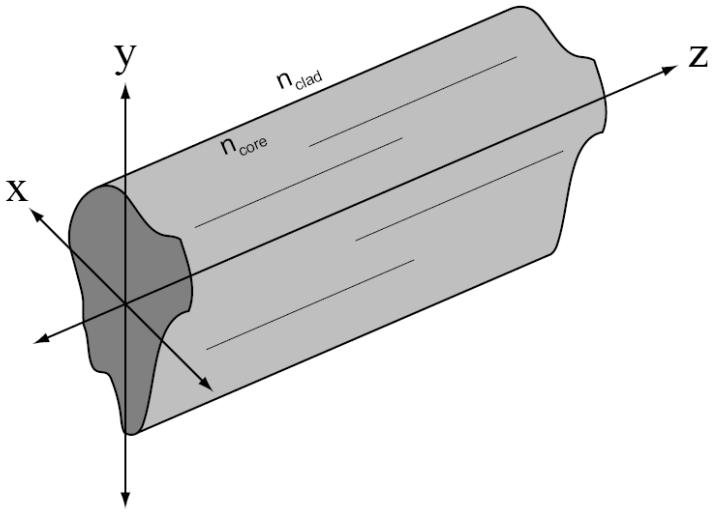

Figure 3.4: Optical waveguide structure

The waveguide is composed of a core region with index of refraction n_{core} surrounded by a cladding region with index n_{clad}. In solving the electric and magnetic fields in a waveguide structure, we first assume solutions which represent travelling waves in the z direction:

$$\mathbf{E}(x, y, z)=\mathbf{e}(x, y)e^{i\beta z}$$
$$\mathbf{H}(x, y, z)=\mathbf{h}(x, y)e^{i\beta z} \quad (19)$$

Where β describes the propagation constant in the z direction. Positive values of β correspond to light propagating in the positive z direction, while negative values of β correspond to light travelling in the reverse direction. When these equations are substituted into

Maxwell's equations (17), the following vector wave equations are obtained after some algebra[28,29,30]:

$$(\nabla_\perp{}^2 + n^2k^2 - \beta^2)\mathbf{e} = -(\nabla_\perp + i\beta\hat{\mathbf{z}})(\mathbf{e}\cdot\nabla_\perp \ln(n^2))$$
$$(\nabla_\perp{}^2 + n^2k^2 - \beta^2)\mathbf{h} = ((\nabla_\perp + i\beta\hat{\mathbf{z}})\times\mathbf{h})\times(\nabla_\perp \ln(n^2)) \quad (20)$$

Equation 20 is the vector wave equation for light propagation in a guiding dielectric structure. The six field components of **e** and **h** in this equation are not independent. Often the index profile n(x,y) is a piecewise constant function, meaning that when viewed in cross section, the waveguide is comprised of a finite number of regions, each of which has a uniform index of refraction. It is a good approximation to treat the index of refraction profile as a series of piecewise constant regions. For cases where the index of refraction can be expressed as a piecewise constant function of x and y, the complicated equation 20 is zero everywhere excepted on the boundary between regions. Within a given region i, it is possible to simpler the equations 20:

$$\left(\nabla^2{}_{xy} + n_i{}^2k^2 - \beta^2\right)\mathbf{e} = 0$$
$$\left(\nabla^2{}_{xy} + n_i{}^2k^2 - \beta^2\right)\mathbf{h} = 0 \quad (21)$$

where n_i is the index of refraction of the i_{th} region. These equations have well know solutions, which can be written in terms of sine's, cosine's, or other harmonic functions. Once the form of the solutions in each region are known, the entire electromagnetic field profile can be found by piecing together the solutions in each region in such a way that the electromagnetic boundary conditions are satisfied at the interface between regions.

The electromagnetic boundary conditions at the interface between two dielectrics can be derived from Maxwell's equations[31]:

$$\begin{aligned}
\left(\mathbf{e}_2 - \mathbf{e}_1\right)\times\hat{\mathbf{n}} &= 0 \\
\left(\mathbf{h}_2 - \mathbf{h}_1\right)\times\hat{\mathbf{n}} &= 0 \\
\left(n_2{}^2\mathbf{e}_2 - n_1{}^2\mathbf{e}_1\right)\cdot\hat{\mathbf{n}} &= 0 \\
\left(\mathbf{h}_2 - \mathbf{h}_1\right)\cdot\hat{\mathbf{n}} &= 0
\end{aligned} \tag{22}$$

The first two equations state that the components of the electric and magnetic field which are parallel to the boundary surface must be continuous. The last two equations state that the normal component of the magnetic field must be continuous across the interface. We can classify the solutions to equation 21 in a given region as either oscillatory or exponential in nature, depending on the value of the propagation constant β. When $\beta<kn_i$, the fields will be oscillatory in nature, expressed for example in terms of sine's, cosine's, etc. When $\beta> kn_i$, the fields will be growing or decaying in nature, expressed for example in terms of exponential functions, hyperbolic functions, etc. Generally, the fields in waveguide structures are oscillatory over a finite region near the center (or core) of the waveguide and decay to zero outside of this region where the surrounding index of refraction is lower. For this reason, all practical waveguide structures consist of a core region surrounded by a cladding region which has a lower index of refraction. In order for the light to be confined or bound in the guiding structure, the propagation constant β must satisfy:

$$n_{clad}k<\beta<n_{core}k \tag{23}$$

where n_{core} and n_{clad} represent the minimum and maximum values of the index refraction profile n(x, y). It can be shown that the modes of a waveguide can be divided into two classes: TE modes, in which $e_z=0$, and TM modes in which $h_z=0$.

There are different kinds of optical waveguide. The optical fiber is used for long distance communication which is engineered so that the structure supports only one bound optical mode for each polarization. The core and cladding regions are both constructed of glass materials and the index change is achieved by modifying the impurities in the glass. Single mode optical fibers typically have core diameters ranging from 3-10 μm, and cladding diameters ranging from 50-125 μm. It is important to recognize that because the circular symmetry of the optical fiber, there is no preferred polarization direction for the fundamental mode. Integrated waveguides differ from fiber-optic cables in that the integrated waveguide is fabricated on a planar substrate using lithographic techniques. This geometry has some advantages over the fiber configuration, the greatest potential advantage being that the optical waveguide could in principle be integrated with other electronic or optical components in the communications system. In addition the planar geometry allows for good control of the waveguide dimensions. However the optical attenuation per unit length of even the best integrated waveguides is still an order magnitude higher than that of optical fiber. One of the simplest waveguide geometries is the channel waveguide, which consists os a rectangular core region, surrounded on all sides by a cladding region.

Glass is often used as the raw material for fabricating passive optical waveguides. One advantage of glass is that it is identical to the materials used construct common optical fibers. Due to the match in index of refraction, it is possible to couple efficiently from a fiber into a glass waveguide. When used for constructing integrated Bragg grating filters, another advantage of using glass waveguides is that they places less of a demand on the nanolithography technology,

3.2.5 Coupling of Modes with a Grating

Now, we consider the problem of a periodic waveguide structure. The modal analysis of waveguides presented in this assumes that the dielectric waveguide is described by an index profile n(x,y) that is independent of z. However, for a grating structure the index of refraction is a periodic function of z. Often, the grating can be treated as a small perturbation on top of an otherwise z-independent waveguide, in which case the effect of the grating is to couple the otherwise independent forward and backwards travelling waves of the waveguide[32]. Coupled mode theory describes how this coupling occurs, and relates the coupling parameters to the geometry of the waveguide and grating. The grating in the surface of a waveguide can be treated as a perturbation of an otherwise uniform waveguide. The unperturbed index of refraction is denoted n(x,y). Generally, the unperturbed waveguide specified by n(x,y) has a series of forward and backward travelling modes.

$$n^2(x,y) \rightarrow \mathbf{e_m}(x,y)e^{i\beta_m z}, \mathbf{h_m}(x,y)e^{i\beta_m z} \tag{24}$$

The perturbed waveguide is described by a modified index of refraction $n^2(x,y)+\delta\varepsilon(x,y,z)$, where $\delta\varepsilon(x,y,z)$ is a perturbation of the waveguide structure. The field solutions for the perturbed waveguide are denoted **E** and **H**.

$$n^2(x,y) + \delta\varepsilon(x,y,z) \rightarrow \mathbf{E}, \mathbf{H} \tag{3.25}$$

In coupled mode theory, we treat **E** and **H**. as a linear superposition of the unperturbed waveguide modes.

$$\begin{aligned} \mathbf{E}(x,y,z) &= \sum_n a_n(z)\mathbf{e_n}(x,y) \\ \mathbf{H}(x,y,z) &= \sum_n a_n(z)\mathbf{h_n}(x,y) \end{aligned} \tag{3.26}$$

The summation index n extends over all of the forward and backward travelling bound modes of the system. For this analysis, we shall take n be a non-zero integer which numbers the bound modes of the waveguide. Negative values of n correspond to backward travelling modes, and positive values of n correspond to forward travelling modes. Coupled mode theory seeks to replace Maxwell's equations with a set of coupled ordinary differential equations describing the coefficients $a_n(z)$. Consider the vector quantity **F**, defined as

$$\mathbf{F} = \left(\mathbf{E} \times \mathbf{h}_{\mathbf{m}}^{*} + \mathbf{e}_{\mathbf{m}}^{*} \times \mathbf{H}\right) e^{-i\beta_m z} \tag{27}$$

em and **hm** are the modal fields of the mth eigenmode of the unperturbed waveguide. These eigenmodes are solutions to Maxwell's equations with the unperturbed index profile n(x,y). Similarly, **E** and **H** are the electromagnetic fields of the perturbed waveguide. If we apply the divergence theorem to the vector **F** over an infinitesimally thin slab which spans the x-y plane at a location z, we arrive at the identity:

$$\frac{\partial}{\partial z} \iint \mathbf{F} \cdot \hat{\mathbf{z}} dA = \iint \nabla \cdot \mathbf{F} dA \tag{28}$$

The divergence term $\nabla \cdot \mathbf{F}$ in the left-hand side of equation 28 can be calculated using equation 3.27, noting that the fields satisfy Maxwell's equations 17:

$$\nabla \cdot \mathbf{F} = ik \sqrt{\frac{\varepsilon_0}{\mu_0}} \delta\varepsilon \mathbf{e}_{\mathbf{m}}^{*} \cdot \mathbf{E} e^{-i\beta_m z} \tag{29}$$

Equation 28 then becomes:

$$\frac{\partial}{\partial z} \iint \mathbf{F} \cdot \hat{\mathbf{z}} dA = ik \sqrt{\frac{\varepsilon_0}{\mu_0}} e^{-i\beta_m z} \iint \delta\varepsilon \mathbf{e}_{\mathbf{m}}^{*} \cdot \mathbf{E} dA \tag{30}$$

The coupled mode equations are found by substituting the mode expansion 26 into equation 30, making use of the orthogonality relationship. This yields:

$$\left(\frac{d}{dz} - i\beta_m\right) a_m(z) = \pm\frac{ik}{4P_m}\sqrt{\frac{\varepsilon_0}{\mu_0}}\sum_n a_n(z)\iint \delta\varepsilon \mathbf{e_n}\cdot\mathbf{e_m}^* dA \tag{30}$$

where the upper sign is used when m represents a forward travelling mode and the lower sign is used when m is negative. Equation 30 describes a system of coupled first order ordinary differential equations which govern the expansion coefficients am(z). Coupled mode theory effectively replaces Maxwell's equations which describe the electromagnetic fields with a series of coupled differential equations which describe how the expansion coefficients evolve. If we let $\delta\varepsilon = 0$ in equation 30, the right-hand side vanishes and the equations of motion become:

$$\left(\frac{d}{dz} - i\beta_m\right) a_m(z) = 0 \tag{31}$$

Thus, in the absence of a perturbation, the expansion coefficients are decoupled, and the solution for $a_m(z)$ is a travelling wave in the z-direction, as expected. For a waveguide that supports only one bound mode, equation 30 reduces to a pair of coupled differential equations which relate the forward and backward travelling mode amplitudes, denoted a+(z) and a–(z):

$$\begin{aligned}\left(\frac{d}{dz} - i\beta\right) a_+(z) &= +ig(z)\left(a_+(z) + a_-(z)\right)\\ \left(\frac{d}{dz} + i\beta\right) a_-(z) &= -ig(z)\left(a_+(z) + a_-(z)\right)\end{aligned} \tag{32}$$

where β is the propagation constant of the forward travelling mode and g(z) is a real-valued, periodic function of z, given by:

$$g(z) = \frac{k}{4P}\sqrt{\frac{\varepsilon_0}{\mu_0}}\iint \delta\varepsilon(x,y,z)\,|\,\mathbf{e}(x,y)\,|^2\,dA \tag{33}$$

For a Bragg grating, the perturbation δε(x,y,z) is a periodic function of z. The function g(z) in equation 33 can be expressed as:

$$g(z) = \begin{cases} K & |z| < \frac{\Lambda}{2}(1-D) \\ 0 & \frac{\Lambda}{2}(1-D) < |z| < \frac{\Lambda}{2} \\ g(z-n\Lambda) & elsewhere \end{cases} \tag{34}$$

where the quantity K is defined as:

$$K = -\frac{k}{4P}\left(n_{core}{}^2 - n_{clad}{}^2\right)\sqrt{\frac{\varepsilon_0}{\mu_0}}\iint_{reticolo} |\,\mathbf{e}(x,y)\,|^2 dA \tag{35}$$

The integral in equation 35 is carried out only over the cross sectional region of the waveguide where the grating is located. Outside of this region, the function δε(x,y,z) is zero. To simplify the coupled mode equations, it is useful to expand the coupling coefficient g(z) in terms of its Fourier components:

$$g(z) = \sum_{n=-\infty}^{\infty} g_n e^{in2\pi\frac{z}{\Lambda}} \tag{36}$$

$$g_n = \frac{1}{\Lambda}\int_{-\frac{\Lambda}{2}}^{\frac{\Lambda}{2}} g(z)e^{-in2\pi\frac{z}{\Lambda}}dz \tag{37}$$

Evaluating the Fourier coefficients in equation 37 gives:

$$g_n = \begin{cases} K(1-D) & n = 0 \\ -\dfrac{K}{n\pi}(-1)^n \sin(n\pi D) & n \neq 0 \end{cases} \tag{38}$$

Substituting the Fourier expansion of equation 35 into the coupled mode equations 32 gives:

$$\begin{aligned} \left(\frac{d}{dz} - i\beta\right) a_+(z) &= +ig_0 a_+(z) + ig_1 a_-(z) e^{+i2\pi\frac{z}{\Lambda}} + \ldots \\ \left(\frac{d}{dz} + i\beta\right) a_-(z) &= -ig_0 a_-(z) - ig_{-1} a_+(z) e^{-i2\pi\frac{z}{\Lambda}} + \ldots \end{aligned} \tag{39}$$

In the above equation, only the significant Fourier terms have been included in each of the coupled mode equations. The effect of the g_0 terms in equation 39 is to slightly modify the propagation constant of the waveguide, so that the perturbed waveguide behaves as if it had a propagation constant β_{new} given by:

$$\beta_{new} = \beta_{old} + g_0 \tag{40}$$

Often the unperturbed waveguide geometry is deliberately chosen so that the 0th Fourier coefficient is zero, in which case there is no first-order change in the propagation constant of the waveguides. In either case, equation 39 reduces to the form:

$$\begin{aligned} \left(\frac{d}{dz} - i\beta\right) a_+(z) &= +ig_1 a_-(z) e^{+i2\pi\frac{z}{\Lambda}} \\ \left(\frac{d}{dz} + i\beta\right) a_-(z) &= -ig_{-1} a_+(z) e^{-i2\pi\frac{z}{\Lambda}} \end{aligned} \tag{41}$$

In the absence of a grating, the solution for a+(z) is $e^{+i\beta z}$ and the solution for a-(z) is $e^{-i\beta z}$. If the grating period is selected so that $\pi/\Lambda \approx \beta$, the grating can cause coupling between the forward and backward modes. The condition $\pi/\Lambda \approx \beta$ is know as the Bragg condition. To complete the analysis, we define the coupling κ in the following way:

$$\kappa = ig_1 = -\frac{ik}{4\pi}\left(n_{core}{}^2 - n_{clad}{}^2\right)\sin(\pi D)\sqrt{\frac{\varepsilon_0}{\mu_0}}\frac{1}{P}\iint_{reticolo} |\,\mathbf{e}(x,y)\,|^2\, dA \tag{42}$$

Substituting equation 41 into 40 gives:

$$\begin{aligned}\left(\frac{d}{dz} - i\beta\right)a_+(z) &= \kappa a_-(z)e^{+i2\pi\frac{z}{\Lambda}} \\ \left(\frac{d}{dz} + i\beta\right)a_-(z) &= \kappa^* a_+(z)e^{-i2\pi\frac{z}{\Lambda}}\end{aligned} \tag{43}$$

The phase of the coupling constant κ in equation 42 depends upon how the grating is placed relative to the z=0 origin. If we consider a guiding structures the bound modes can be sufficiently described with a single scalar quantity $\Phi(x,y)$, representing one of the transverse field components of the mode. Then, the bound power P of the mode is given by:

$$P = \frac{\beta}{2k}\sqrt{\frac{\varepsilon_0}{\mu_0}}\iint |\,\Phi(x,y)^2 dA \tag{44}$$

By substituting the above equation into equation 42 we obtain the following expression for the grating strength κ in terms of the scalar field $\Phi(x,y)$:

$$\kappa = \frac{k^2}{2\pi\beta}\left(n_{core}{}^2 - n_{clad}{}^2\right)\sin(\pi D)\Gamma \tag{45}$$

where the quantity Γ is a dimensionless overlap integral given by:

$$\Gamma = \frac{\iint_{reticolo} |\Phi(x,y)|^2 \, dA}{\iint |\Phi(x,y)|^2 \, dA} \tag{46}$$

The factor Γ defined in equation 46 is a measure of how much the optical mode overlaps with the grating region. The integral in the numerator of equation 46 is carried out only over the grating region whereas the integral in the denominator extends over the entire cross-sectional plane.

3.3 Ion-Exchanged Glass Waveguide

Ion exchange has been considered one of the most important techniques for glass waveguide fabrication[33] for integrated optical devices, such as wavelength division multiplexer/demultiplexer, the power splitter/combiner, and the optical filter. A two-step K^+-Na^+ and Ag^+-Na^+ ion-exchange technique is introduced to fabricate single-mode channel waveguides in BK7 glass for the telecom-wavelength region. During the first ion-exchange step, bare glass wafers are dipped into a pure KNO3 melt to conduct the K^+-Na^+ ion exchange. The Na^+ ions in the surface region of the glass will be interchanged by the K^+ ions from the KNO3 melt through thermal diffusion. The K^+ ions will cause a higher refractive index than the Na^+ ions. The ion-exchange temperature and the time of this step must be chosen to make sure that the depth and the refractive-index increase in the K^+ ionic layer are not large enough to support any waveguide mode. After the first ion-exchange step, a standard photolithography process is applied to constructing masking patterns on the glass wafers.

Then we immerse these glass wafers into an AgNO3 melt to perform the Ag^+-Na^+ ion exchange. In fact, during the first step, the K^+-Na^+ ion exchange is not complete; a small percentage of the Na^+ ions is left in the K^+ layer. Therefore the Ag^+ ions can diffuse into the glass in the unmasked regions through the K^+ layer. Usually the temperature during the second step is much lower than that of the first step, at which the diffusivity of the K^+ ions is very low; thus the K^+ ionic layer does not change during this step. Because the Ag^+ ions cause a much higher refractive index increase than the K^+ ions, the index peak is actually below the K^+ ionic layer. As a result, buried waveguides are obtained.

3.4 A Waveguided Tunable Bragg Grating Using Composite Materials

A novel, compact and low cost tuneable and switchable guided wave optical filter using a holographic Bragg grating as the optic field perturbation element has been realized. The grating is made by alternate μ-slices of cured UV polymers and electrically controlled nematic liquid crystals, known as POLICRYPS[9] (POlymer LIquid CRYstal Polymer Slices) and it is used as overlayer of a double ion-exchanged glass single mode channel optical waveguide. We use a K^+-Na^+/Ag^+-Na^+ double ion-exchanged process in BK7 glass to obtain low losses (< 1 dB/cm) and high index-contrast ($\Delta n \cong 0.04$) optical waveguides

.

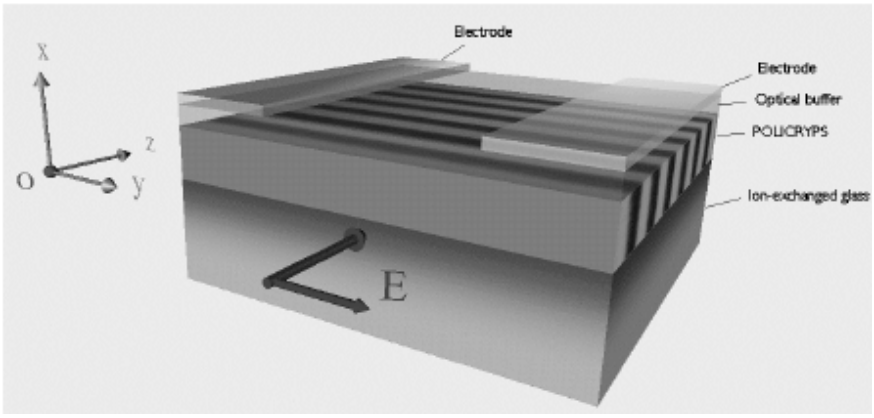

Figure 3.5: Tridimensional view of a waveguided optical filter using POLICRYPS grating as a cladding of an ion-exchanged optical waveguide.

The structure of the device, sketched in Figure 3.5, includes coplanar electrodes deposited above an optical buffer, consisting of a spin-on-glass material, which has a refractive index of 1.4. The optical buffer is assumed thick enough so that the effects of the electrodes on the propagation of light can be neglected.

The polymer used for the POLICRYPS is NOA 61, whose refractive index at λ_0= 1550 nm is n_P= 1.5419, and the NLC is 5CB, whose ordinary and extraordinary refractive indices are respectively 1.5108 and 1.6807 at 20°C. The waveguide is monomode at λ_0= 1550 for refractive index of the NLC near to the one of the polymer. The boundary conditions imposed by the confining walls of the polymers in the POLICRYPS ensures that the LC alignment is along the z-axis as illustrated in figure 3.6

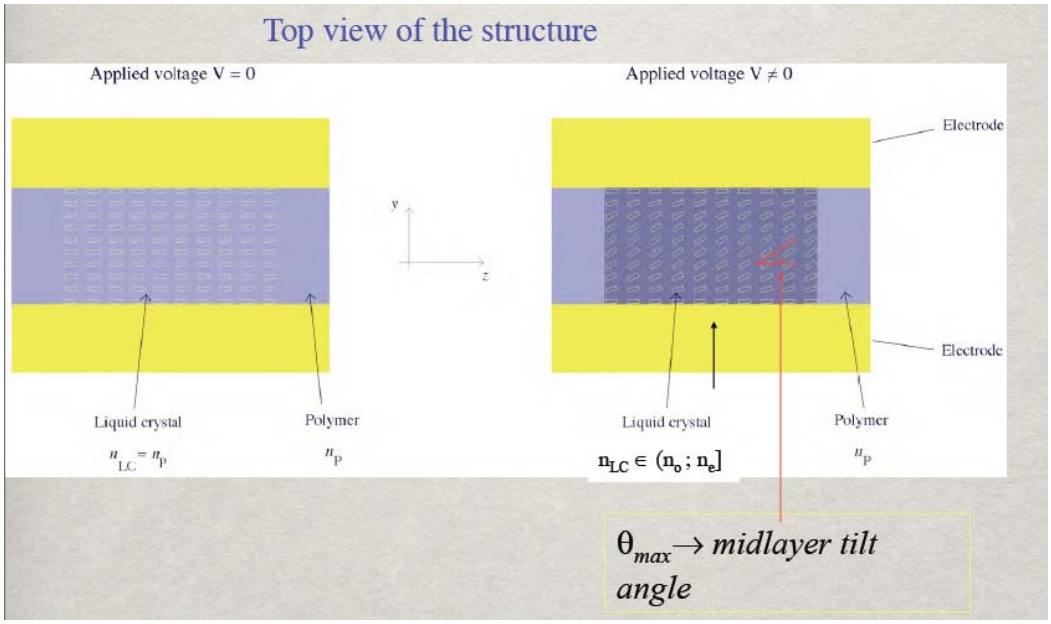

Figure 3.6: Top view of the filter showing the polymer-liquid crystal interface both without and with applied voltage.

In fact in the absence of external electrical field, the director of the LC molecules is aligned orthogonally to the Polymer/LC interface (homeotropic alignment). A TE optical field propagating along (O*z*) will see the ordinary index *n*o of the NLC. Applying an external electrical field (see right-hand side of Figure 3.6), the molecules rotate in the plane (*yz*) and the TE optical field will see a refractive index n between *n*o and *n*e.

The index mismatch between the polymer and liquid crystal slices can be varied by varying the external electrical field, letting the Bragg grating appear and opening a photonic band gap in the transmission curve. The index mismatch influences the optical path length therefore the position of the gap given by the Bragg relation, $m\lambda=2n\Lambda$, m being the grating order, n being an average refractive index and Λ being the grating period, the gap width and the transmission minimum. Figure 3.7 shows the optical setup used to investigate the optical propagation through the filter and in particular to evaluate the reflection optical response.

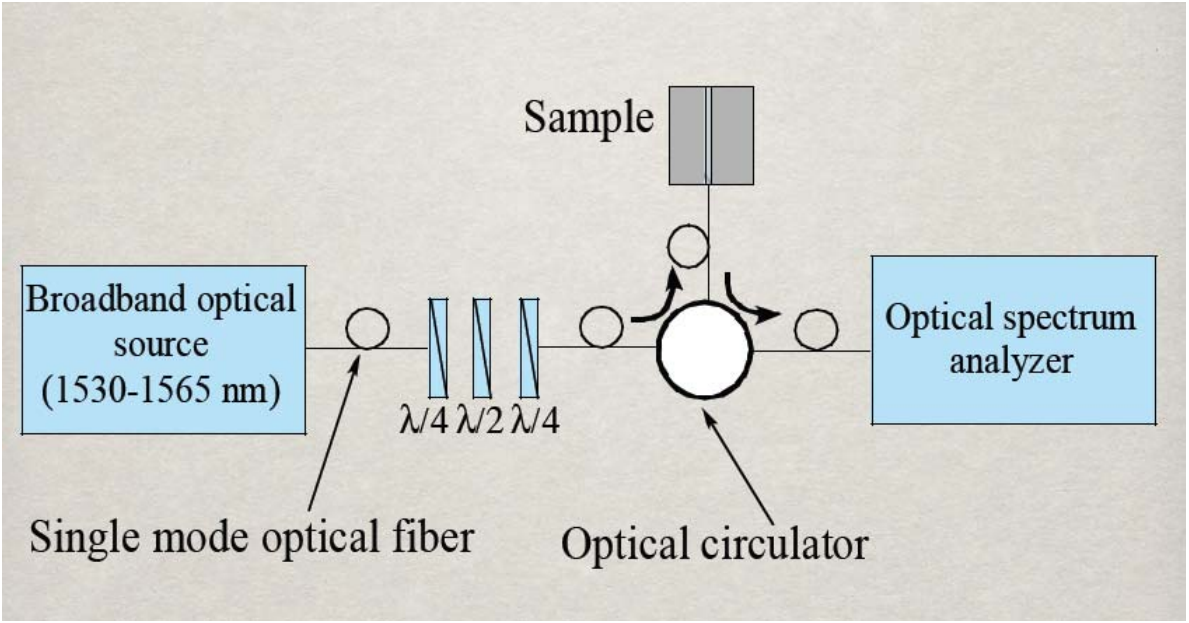

Figure 3.7:. Set-up for the reflection optical response of the filter

A broadband source based on spontaneous emission of an erbium doped fiber amplifier was connected to a pigtailed polarization controller in order to characterize the optical response of the filter in the 1530-1565 nm band. The polarization controller consists in a series of three waveplates, a half wave plate sandwiched between two quarter wave plates, which allow to linearly polarize the broadband source light signal and to rotate the polarization without power variation.

The optical signal coming from the second port of the circulator was connected to a single mode optical fiber, terminated with a cleaved face to couple light into the guided wave optical filter. The signal reflected by the filter, is routed to an optical spectrum analyzer by the circulator through its third port. The transmission spectrum was obtained by coupling both the filter input and output to two cleaved fibers without using the circulator. Before coupling the cleaved fiber with the optical filter, the state of light polarization injected into the sample was measured by means of a polarizer.

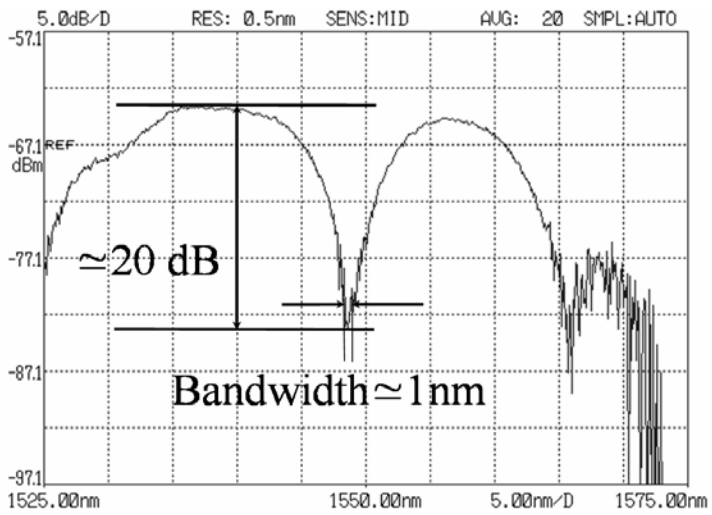

Figure 3.8: Typical filter optical transmittance measured response. by means of an optical spectrum analyzer.

Figure 3.8 shows a typical transmission spectral response of this novel tuneable optical filter with a 20 dB suppressed signal at the designed Bragg wavelength of 1549 nm with a band at –17 dB of about 1 nm. By applying a square wave voltage of 1 kHz to the filter electrodes, tuning of the optical response was observed.

Figure 3.9 shows the reflection optical response of the filter for different driving voltages.

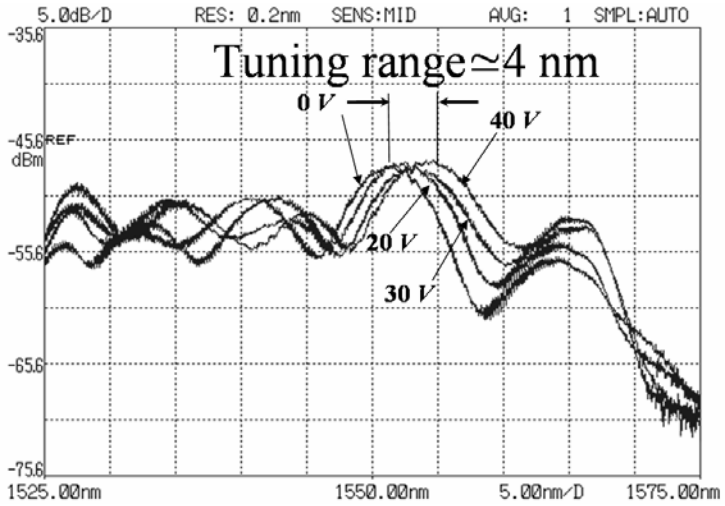

Figure 3.9: Tuning of the filter reflection response

A tuning range of ≅ 4 nm was obtained by applying a square wave of about 40V of amplitude. The resulting device is the demostration of a simple and inexpensive technology to make integrated optic functional components on glass.